Ordering Behavior of the Two-Dimensional Ising Spin Glass with Long-Range Correlated Disorder

L. Münster,[1] C. Norrenbrock,[1] A. P. Young,[2] and A. K. Hartmann[1, *]

[1]*Institut für Physik, Universität Oldenburg, 26111 Oldenburg, Germany*
[2]*University of California Santa Cruz, CA 95064, USA*
(Dated: January 18, 2021)

The standard two-dimensional Ising spin glass does not exhibit an ordered phase at finite temperature. Here, we investigate whether long-range correlated bonds change this behavior. The bonds are drawn from a Gaussian distribution with a two-point correlation for bonds at distance r that decays as $(1 + r^2)^{-a/2}$, $a \geq 0$. We study with exact algorithms numerically the ground state and domain wall excitations. The results indicate still the absence of spin-glass order at any finite temperature. A further analysis reveals that the correlation has strong effects on local length scales inducing ferro/antiferromagnetic domains into the system. The length scale of ferro/antiferromagnetic order diverges exponentially as the correlation exponent approaches a critical value, $a \longrightarrow a_{\mathrm{crit}} = 0$. Thus, our results suggest that the system becomes a ferro/antiferromagnet only in the limit $a \to 0$.

I. INTRODUCTION

Spin glasses are disordered magnetic materials which exhibit peculiar properties at very low temperatures [1]. To understand these materials, the Edwards-Anderson (EA) model and the Sherrington-Kirkpatrick (SK) model [2, 3] have been developed. Spin glasses exhibit essential aspects of complex behavior [4] and research on spin glasses [5–7] has stimulated progress in numerous other fields, such as information processing [8], neuronal networks [9], discrete optimization [10, 11] or Monte-Carlo simulation [12].

In this work we study the two-dimensional EA model with Ising spins commonly referred to as two-dimensional Ising spin glass. It exhibits Ising spins with short-range quenched random pair-wise interactions, for details see Sec. II. Its properties are well described in the framework of the scaling/droplet picture [13–15], as has been confirmed by numerical droplet calculations for large systems with exact ground-state algorithms [16, 17]. The model exhibits no finite-temperature spin glass phase in contrast to the three or higher dimensional variants [18–20]. At the zero-temperature phase transition the distribution of the interaction disorder has some influence on some critical properties. The investigation of similarities and differences between continuous Gaussian and discrete bimodal $\pm J$ disorder were the origin of intensive research [21–24]. Since the non-existence of a finite-temperature spin-glass phase for short range two-dimensional models is independent of the disorder distribution, we consider here only the Gaussian case. Previous works have shown how the manipulation of the mean of the Gaussian from zero to a sufficiently large value, or the introduction of other sufficient majorities of the ferromagnetic interactions, causes a ferromagnetic phase [25–29]. In this work

we address the question how long-range correlated disorder impacts the ordering behavior, in particular wether it leads to a low-temperature spin-glass phase. Here, long-range means that the correlation decays with a power law such that it is not bound to a certain length scale. In other disordered systems the subject of long-range correlation has already been taken into account [30]. Our study was partially motivated by a corresponding numerical study for the three-dimensional random-field Ising model with long-range correlation [31], where an influence on the quantitaive ordering behavior has been observed for some critical exponents and in the case of strong correlation. Note that the case of the random-field model is a bit different, because the correlation acts on the local random fields which work for the independent randomness case against the ferromagnetic order. Consequently, from an extended Imry-Ma argument it was predicted [32] that the random-field Ising model with strong long-range correlation is expected to show an increase of the lower critical dimension of the ferromagnetic order, opposite to what may be expected for the spin-glass case.

The following content is structured into three parts. First, the model is introduced and it is outlined how ground state computations under changing boundary conditions are used to inflict domain wall excitations. Second, the results of the simulations will be presented. We finish by a discussion.

II. MODEL AND METHODS

A. The Ising Spin Glass with Correlated Bonds

The Ising spin glass consist of Ising spins $s_{\boldsymbol{m}} \in \{\pm 1\}$ on the sites $\boldsymbol{m} \in \Lambda$ of a two-dimensional lattice, i.e. $\Lambda \subset \mathbb{Z}^2$. In this study only quadratic systems are considered, such that the spin glass has L spins in each direction and
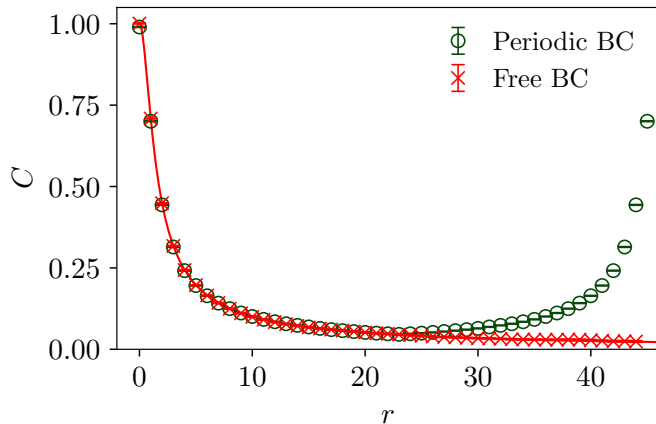
FIG. 1. (color online) Correlation of the bonds of a spin glass, calculated with Eq. (3), with $a = 1$ and $L = 46$ spins in each direction, x and y. The system has free boundary conditions in one direction and periodic boundary conditions in the other direction. The bond correlation was generated according to the FFM with periodic boundary conditions in both directions, but the size in the directions of free boundaries was chosen much larger than the corresponding system size L. The line follows a fit of type $B_C(1 + r^2)^{-A_C/2}$, yielding $B_C = 1.0003(12)$ and $A_C = 0.9953(13)$. The average was taken over 10000 realization of the disorder. The good agreement proves that the generation of the randomness works well.

$|\Lambda| = L^2$. The Hamiltonian is given by

$$H_{\boldsymbol{J}}(\boldsymbol{s}) = -\sum_{\{\boldsymbol{m},\boldsymbol{n}\} \in \mathcal{M}} J_{\boldsymbol{m},\boldsymbol{n}} s_{\boldsymbol{m}} s_{\boldsymbol{n}}, \qquad (1)$$

where the sum runs over all nearest-neighbor spin sites $\mathcal{M} = \{\{\boldsymbol{m},\boldsymbol{n}\} : \|\boldsymbol{m}-\boldsymbol{n}\| = 1 \wedge \boldsymbol{m},\boldsymbol{n} \in \Lambda\}$. The bonds, $J_{\boldsymbol{m},\boldsymbol{n}}$, which represent the interaction between two spins, are random in strength and sign but remain constant over time. Hence, one speaks of a quenched disorder when the system is investigated under a fixed realization of the bonds, $\boldsymbol{J}$. Here, the bonds originate from a continuous correlated Gaussian random field, $J(\boldsymbol{x})$, with zero mean, $\langle J(\boldsymbol{x}) \rangle = 0$, and a covariance that reads as

$$\langle J(\boldsymbol{x})J(\boldsymbol{x}+\boldsymbol{r}) \rangle = (1 + r^2)^{-a/2}, \qquad (2)$$

$\boldsymbol{x}, \boldsymbol{r} \in \mathbb{R}^2$, $a \geq 0$ and $r = \|\boldsymbol{r}\|$. The entries of $\boldsymbol{J}$ are given by, $J_{\boldsymbol{m},\boldsymbol{n}} = J((\boldsymbol{m}+\boldsymbol{n})/2)$, which ensures that the correlation decays in the same manner along both axes. The correlation exponent, a, is the only parameter to control the correlation. For $a = 0$ one obtains the Ising model of a ferromagnet or antiferromagnet, respectively, depending on the bond realization. When $a \longrightarrow \infty$ the uncorrelated Ising spin glass model with Gaussian disorder is recovered.

To generate the correlated bonds numerically we utilized the Fourier Filtering Method (FFM) [31, 33]. The FFM is a procedure to create stationary correlated random numbers of previously independent random numbers. Because it is based on the convolution theorem it is

possible to benefit from the computational efficient Fast Fourier Transform Algorithm [34]. For its implementation we relied upon the functions of the FFTW library, version 3.3.5 [35]. Figure 1 shows the average bond correlation along the main axes of a system with $|\Lambda| = 46^2$ spins calculated by the estimator,

$$C(\boldsymbol{r}) = \frac{1}{|\mathcal{M}'|} \sum_{\{\boldsymbol{n},\boldsymbol{m}\} \in \mathcal{M}'} \langle J_{\boldsymbol{m},\boldsymbol{n}} J_{\boldsymbol{m}+\boldsymbol{r},\boldsymbol{n}+\boldsymbol{r}} \rangle_J . \qquad (3)$$

$\langle ... \rangle_J$ denotes the average with respect to the disorder. $\mathcal{M}' \subset \mathcal{M}$ is adapted to the boundary conditions (BCs).

B. Ground States and Domain Walls

The nature of the ground state (GS) of the two-dimensional Ising spin glass is an intriguing subject on its own [36, 37]. Beside that, GS computations of finite systems are a well established tool [10, 11] to investigate the glassy behavior of the model in the zero-temperature limit [38]. The GS is the spin configuration which minimizes Eq. (1) for a given realization of the bonds. In case of two-dimensional planar lattices there exist exact procedures to generate the GS with a polynomial worst-case running time. This is in contrast to the three or higher-dimensional variants which belong to the class of NP-hard problems [39]. In fact, there is more than one approach to compute the GS such as the algorithm of Bieche *et al.* [40] or Barahona *et al.* [41]. The key idea of these algorithms is to create a mapping from the original problem defined on the underlying lattice graph of the spin glass onto a deduced graph which is constructed in such a manner that the GS can be extracted from a *minimum-weight perfect matching*, which is polynomially computable. In this work we applied an ansatz which includes Kasteleyn-city subgraphs into the mapping process and thus is more efficient [42, 43] in terms of speed and memory usage than the above mentioned algorithms. This allowed us to investigate systems up to a linear system size of $L = 724$ spins in each direction with decent computational resources. For the computation of the minimum-weight perfect matching the Blossom IV algorithm [44] implemented by A. Rohe [45] was utilized.

To study the spin glass at nonzero temperature we inflict domain wall (DW) excitations into the system. This was done by computing GSs under periodic and antiperiodic BCs also referred to as P-AP [46]. It works as follows: First, a spin glass with periodic BCs in one direction and free BCs in the other direction is generated under a quenched disorder, $\boldsymbol{J}^{(\mathrm{p})}$. Then, its GS configuration, $\boldsymbol{s}_{\mathrm{gs}}^{(\mathrm{p})}$, is computed. Now, the periodic BCs are replaced by antiperiodic BCs, by reversing the sign of one column of bonds parallel to the direction of periodicity, which leads to $\boldsymbol{J}^{(\mathrm{ap})}$. Afterwards, the new GS configuration, $\boldsymbol{s}_{\mathrm{gs}}^{(\mathrm{ap})}$, is calculated. The change of the BCs imposes a DW of minimal energy between the two spin configurations $\boldsymbol{s}_{\mathrm{gs}}^{(\mathrm{p})}$ and $\boldsymbol{s}_{\mathrm{gs}}^{(\mathrm{ap})}$. The energy of the DW is given

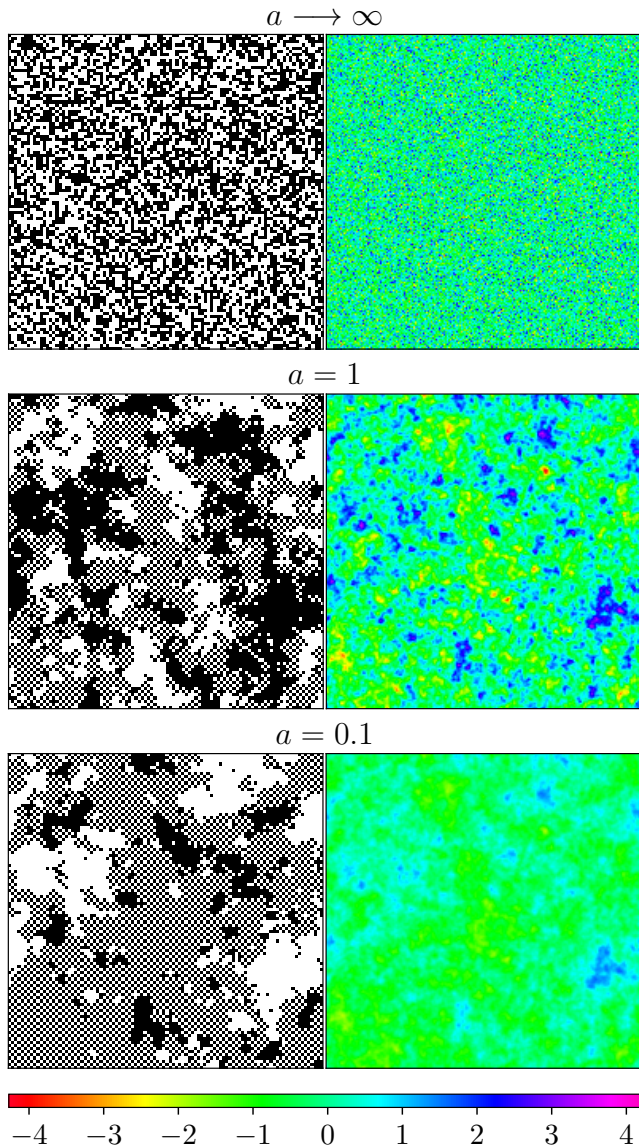$a \longrightarrow \infty$

$a = 1$

$a = 0.1$

FIG. 2. (color online) The right hand side of the figure shows one realization of the discretized Gaussian random field, from which the bonds are extracted, for three different correlation exponents. The corresponding GSs are on the left. The correlations exponents are given by $a \longrightarrow \infty$ (top), $a = 1$ (center) and $a = 0.1$ (bottom). Black points denote $s_{\boldsymbol{m}} = -1$ and white points $s_{\boldsymbol{m}} = 1$. In ferromagnetic order two neighboring spins have same sign and in antiferromagnetic order the sign alternates. The system size is $L = 100$.

by

$$\Delta E = H_{\boldsymbol{J}^{(\mathrm{ap})}}\left(\boldsymbol{s}_{\mathrm{gs}}^{(\mathrm{ap})}\right) - H_{\boldsymbol{J}^{(\mathrm{p})}}\left(\boldsymbol{s}_{\mathrm{gs}}^{(\mathrm{p})}\right). \qquad (4)$$

The geometrical structure of a DW can be characterized by the number $\mathcal{D}_L$ of bonds which are included in the surface. To avoid including those bonds which are a direct result of the different BCs, the surface is defined to consist of those bonds which fulfill

$J_{\boldsymbol{m},\boldsymbol{n}}^{(\mathrm{p})} s_{\boldsymbol{m}}^{(\mathrm{p})} s_{\boldsymbol{n}}^{(\mathrm{p})} J_{\boldsymbol{m},\boldsymbol{n}}^{(\mathrm{ap})} s_{\boldsymbol{m}}^{(\mathrm{ap})} s_{\boldsymbol{n}}^{(\mathrm{ap})} < 0$, where $\boldsymbol{m}, \boldsymbol{n}$ runs over all unordered pairs of nearest neighbor lattice sites [21].

III. RESULTS

We have obtained exact ground states for systems with correlation exponents in the range $a \in [10^{-3}, \infty]$, where $a = \infty$ corresponds to independently sampled bonds. Since the GS calculation requires only polynomial time as a function of the system size, we were able to study sizes up to a large value of $N \equiv L^2 = 724^2$ for each value of a. For each combination, we performed an average over the realizations of the disorder, ranging from 10^6 realizations for the smallest sizes up to 10000 realizations for $L = 512$ and 2000 realizations for the largest system size.

Figure 2 provides a first impression how the bond correlation impacts the ordering of the GS. On one hand, it is visible that for strong correlations there are large areas where the spins are either in ferromagnetic or antiferromagnetic order. On the other hand, there are large areas where, due to the correlation, the bonds have identical sign and similar absolute value.

A. Domain Wall Energy

Next, we look at the influence of the bond correlation on the properties of the previously discussed DW excitations. The absolute value of the DW energy is proportional to the coupling strength between block spins in the zero-temperature limit [14]. A stable order is possible if the average absolute value of the DW energy increases with the system size. In the uncorrelated case, $a \longrightarrow \infty$, one obtains a power law behavior [14, 20, 21, 47],

$$\langle |\Delta E| \rangle_J \sim L^\theta, \qquad (5)$$

where θ is the stiffness exponent with its current best estimate $\theta = -0.2793(3)$ [21]. Since $\theta < 0$ there is no stable spin-glass phase for temperatures larger than zero. Figure 3 shows the impact of the correlation on the scaling of $\langle |\Delta E| \rangle_J$. For $a \geq 0.9$ one can still observe the pure power-law decay of the uncorrelated model on sufficiently long length scales. The inset demonstrates that the stiffness exponent stays constant with respect to the value of the uncorrelated model. For values of $a \leq 0.9$ the average $\langle |\Delta E| \rangle_J$ initially grows with system size, but starts decrease for larger system, i.e. the curves exhibit a peak. The system size L^* where the peak occurs shifts to larger system sizes by decreasing the correlation exponent a. This will be analyzed below.

Before this, we show the results for the average DW energy $\langle \Delta E \rangle_J$, which behaves in a similar manner as the absolute value, as it is shown in figure 4.

If spin-glass order existed in this model for some value of a one would observe an increase $\langle |\Delta E| \rangle_J$ in the limit
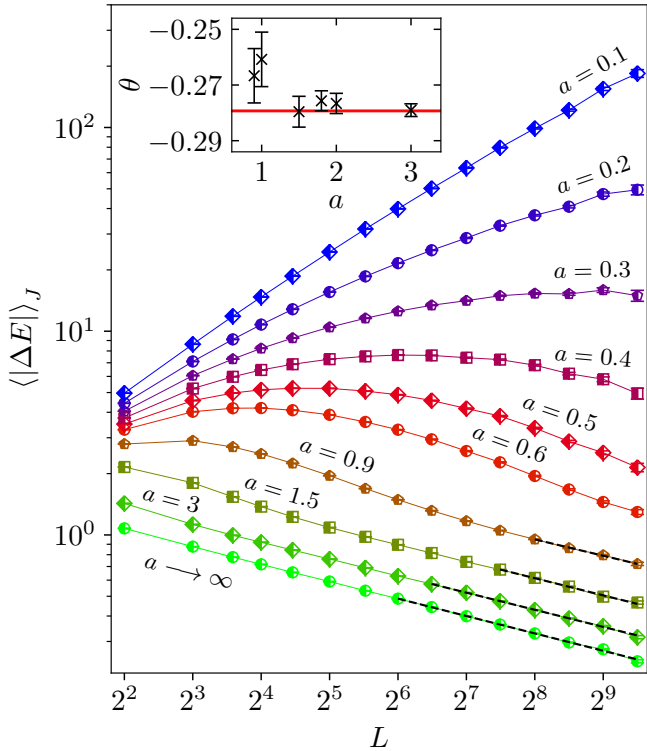
FIG. 3. (color online) Scaling of the absolute value of the DW energy as a function of system size L for different values of a. The full lines are guides to the eyes only. The broken lines are fits of type $\langle|\Delta E|\rangle_J = A_\theta L^\theta$. The inset shows the values of θ which were obtained by fits for values of $a \geq 0.9$. The red line marks the value of the stiffness exponent for $a \longrightarrow \infty$ according to [21].
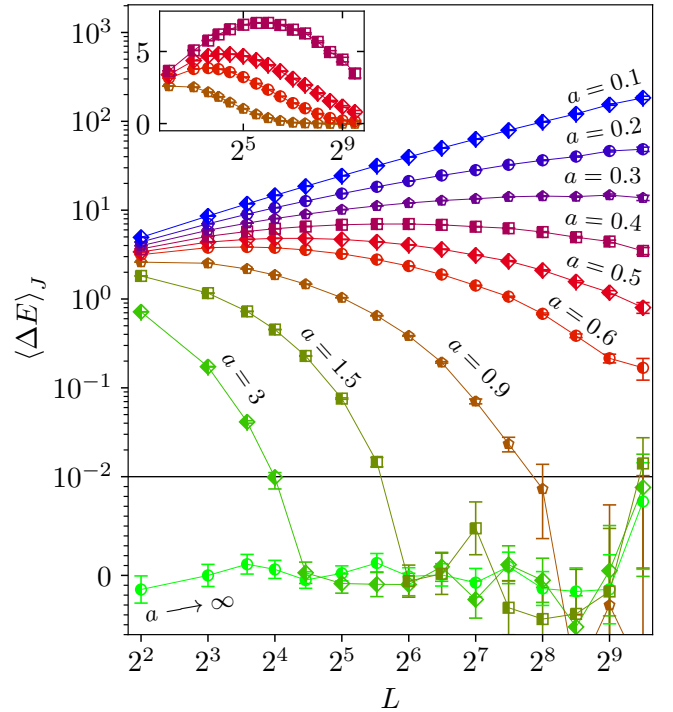

FIG. 4. (color online) A log-log plot of the DW energy $\langle\Delta E\rangle_J$ as a function of the system size L for some values of correlation exponent a. The inset shows the same data with linear energy scale for $a = 0.4$, 0.5, 0.6 and 0.9 to highlight the peak structure. The lines are guides to the eyes only.

$L \to \infty$, while at the same time $\langle\Delta E\rangle_J$ would remain at or converge to zero as a function of L. The latter one would indicate the absence of a simple ferromagnetic order, because for a spin glass the change of the boundary conditions from periodic to antiperiodic is symmetric, i.e., could either increase or decrease the GS energy. The, possible only partial, increase of both $\langle|\Delta E|\rangle_J$ and $\langle\Delta E\rangle_J$ for small values of L and A corresponds to a ferro/antiferromagnetic ordering on local length scales, which is visible in Fig. 2 and will be discussed more below. Whether there may be an ordered phase for very small values of a, is discussed next.

To track how the length scale of local order changes in dependency of the correlation strength we measure the peak lengths L^*, for the domain-wall energy and the absolute value, respectively, as a function of the correlation exponent a. Numerically, L^* was computed by fitting parabolas in the vicinity of the peaks of $\langle|\Delta E|\rangle_J$ and $\langle\Delta E\rangle_J$. As the fit in figure 5 demonstrates the data for $L^*(a)$ is well described by an exponential function

$$L^*(a) = A_L \exp\left\{b_L (a - a_{\mathrm{crit}})^{-c_L}\right\}. \qquad (6)$$

Nonzero values of a_{crit} would indicate that for $a < a_{\mathrm{crit}}$ an ordered phase exisits. A true spin-glass phase would be possible if a_{crit} for $\langle\Delta E\rangle_J$ is smaller than a_{crit} for $\langle|\Delta E|\rangle_J$. We obtained values of $a_{\mathrm{crit}} = 0.13(0.10)$ for $\langle\Delta E\rangle_J$ and $0.10(0.17)$ for $\langle|\Delta E|\rangle_J$ with quality of the fit $Q = 0.87$ and $Q = 0.58$, respectively. Thus, zero values for the critical correlation exponents seem possible. To evaluate this, we set a_{crit} to zero and obtain the values of the other fit parameters, which here are $A_L = 3.63(22)$, $b_L = 0.39(4)$, $c_L = 2.10(6)$ $(Q = 0.86)$ for $\langle\Delta E\rangle_J$ and $A_L = 3.5(4)$, $b_L = 0.55(6)$, $c_L = 1.85(8)$ $(Q = 0.63)$ for $\langle|\Delta E|\rangle_J$. Since the qualities of the fits remain almost identical in comparison to $a_{\mathrm{crit}} \neq 0$ the data is considered to be consistent with $a_{\mathrm{crit}} = 0$, which would imply that there is no global order when $a > 0$, let it be ferromagnetic or spin glass. The inset shows that the behavior of $L^*(a)$ is also compatible with $c_L = 2$. Fits of this type, with $a_{\mathrm{crit}} = 0$ and $c_L = 2$ fixed, have quality of the fit larger than 0.4, which is reasonable. Note that an exponential dependence of the "breakup" length scale of ferromagnetic order as a function of disorder strength was also found in the two-dimensional random field Ising model, at low temperatures [48] and for the GS [49].
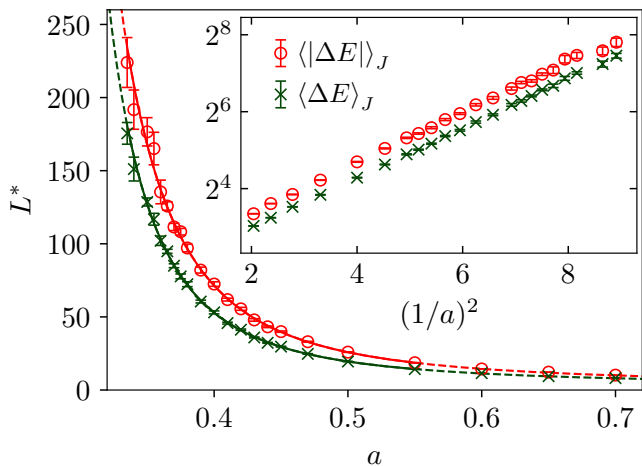
FIG. 5. (color online) The system size where the peak of $\langle|\Delta E|\rangle_J$ and $\langle\Delta E\rangle_J$ occurs, denoted as L^*, as a function of a. The lines are fits according to Eq. (6) in the range $a \leq 0.55$, see text for details. The broken lines are extrapolations of the fits. The inset shows L^* on a logarithmic scale as a function of $1/a^2$ exhibiting a straight-line behavior, and thus confirming the behavior obtained from the fit.
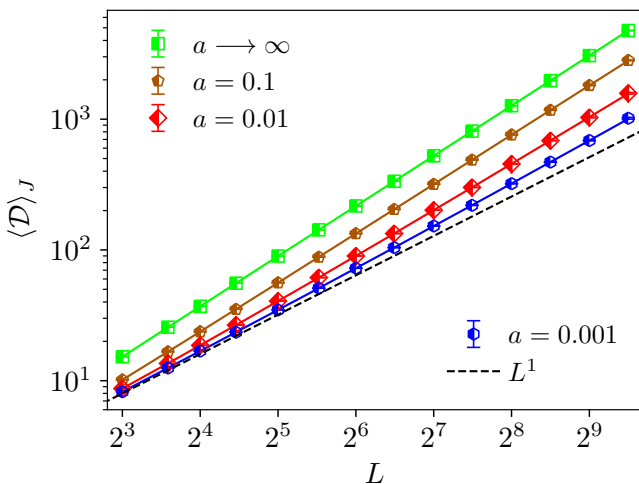

FIG. 6. (color online) Scaling of the DW surface $\langle\mathcal{D}\rangle_J$ for different values of a. The broken black line shows the scaling of the DW surface in case of a ferro/antiferromagnet. The full lines follow fits according to Eq. (8) with $L_{\min}^{(\mathrm{fit})} = 8$.

B. Domain Wall Surface

The behavior of DW surfaces is regarded as one of the essential parameters which describe the properties of random systems [50, 51]. DWs separate spins in GS and reversed GS. Their surface is defined as those bonds which belong to the DW, we denote the size as $\mathcal{D}$. In the uncorrelated case, $a \longrightarrow \infty$, the average DW surface size
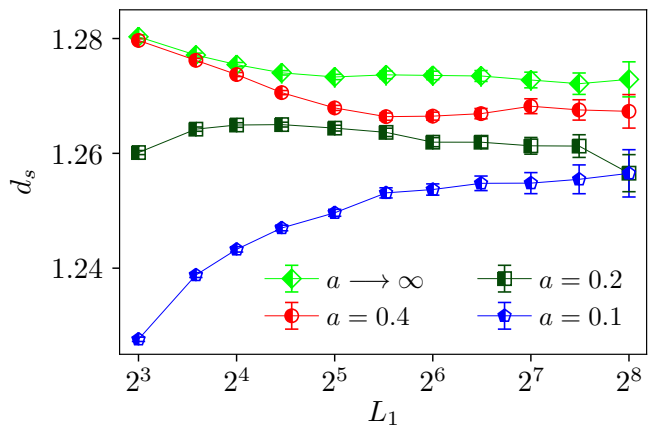

FIG. 7. (color online) The fractal surface dimension of the DW surface d_s as a function of the smallest system size L_1 of a fit window.

exhibits a power law [52, 53],

$$\langle\mathcal{D}\rangle_J \sim L^{d_s}, \tag{7}$$

where d_s is the fractal surface dimension, which the so-far best numerical estimate $d_s = 1.27319(9)$ [21]. When $a = 0$ the system is a ferro/antiferromagnet and $\langle\mathcal{D}\rangle_J = L$, implying that $d_s = 1$, i.e., the surface is not fractal here. Figure 6 shows the scaling of the DW surface size for different values of a. In general, it can be seen that the correlation decreases the number of bonds in the DW surface. For $a = 0.001$ the data shows already a visible a visible deviation from the linear behavior on the double-logarithmic scale. To study this behavior we fitted pure power-laws to the data. For this purpose, we did not a full fit to all data points, but used the sliding-window approach instead. Here, four values of $\langle\mathcal{D}\rangle_J$ which are adjacent in terms of system size were grouped together in one fit window, respectively. The independent variables of such a fit window were given by (L_1, L_2, L_3, L_4) with $L_i < L_{i+1}$, $i = 1, ..., 4$. The dependent variables corresponded to the data, i.e. $\langle\mathcal{D}_{L_i}\rangle_J$. The smallest independent variable of each fit window is denoted as L_1. For each window, we fitted the power law to the data resulting in a value of d_s. The dependence of d_s as a function of L_1 for different values of a can be found in figure 7. In the uncorrelated case d_s decreases as a function of L_1, whereas for strong correlations d_s increases. In any case, for system sizes $L_1 < 32$ and small values $a \leq 1$ we observed some notable dependence of d_s on the system size. This motivated us to include corretions to scaling int the power law Eq. (7) by considering [16, 21]

$$\langle\mathcal{D}\rangle_J = A_\mathcal{D} L^{d_s}(1 + B_\mathcal{D} L^{-\omega_s}) . \tag{8}$$

By using Eq. (8) the quality of the fit is larger than 0.79 for all studied values of $a \leq 0.1$ with smallest linear system size of the fit $L_{\min}^{(\mathrm{fit})} = 8$. For larger values of a, the
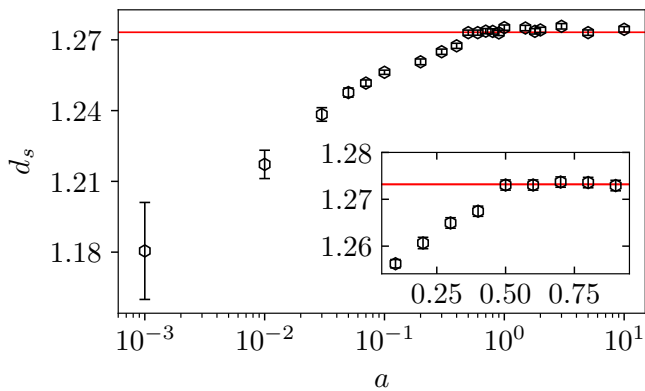
FIG. 8. (color online) The fractal surface dimension as a function of a. The values for $a \geq 0.2$ were obtained by pure power law fits, i.e. $\langle \mathcal{D} \rangle_J = A_{\mathcal{D}} L^{d_s}$ with smallest considered system size $L_{\min}^{(\mathrm{fit})} = 128$. The values for $a \leq 0.1$ were received by fits to Eq. (8) with $L_{\min}^{(\mathrm{fit})} = 8$. The red line marks the value of d_s for $a \longrightarrow \infty$ according to [21].

pure linear fit was always fine, given our statistical accuracy. Figure 8 shows the resulting fractal surface dimension for all considered values of a. At $a \approx 0.4$ the fractal surface dimension starts to decline from $d_s = 1.27319(9)$ [21], in the uncorrelated case, to smaller values. This is also visible in Fig. 7. Thus, it appears that for small values of a the fractal structure of the cluster changes, altough there is no phase transition. Note that we also performed fits (not shown) of power laws plus a constant, the extrapolated fractal dimension, to the sliding window fractal dimensions shown in Fig. 7. The behavior of this extrapolated fractal dimension also exhibits the same notable decrease of d_s for $a \leq 0.4$. Of course, it can not be ruled out that on sufficiently large, i.e., much larger than currently accessible, length scales the fractal dimension of the uncorrelated model is recovered again and thus $d_s = 1.27319(9)$ [21] for all values $a > 0$.

C. Ground State Correlation

In the following, the impact of the bond correlation on the spin correlation of the GS will be discussed. Note that at zero temperature there is no thermal disorder and for our study the is not degenerate, i.e., unique. The two-point spin correlation is given by $\langle s_{\boldsymbol{m}}^{(\mathrm{gs})} s_{\boldsymbol{m}+\boldsymbol{r}}^{(\mathrm{gs})} \rangle_J$, where $s_{\boldsymbol{m}}^{(\mathrm{gs})}$ denote spins in GS configuration. In the uncorrelated model $\langle s_{\boldsymbol{m}}^{(\mathrm{gs})} s_{\boldsymbol{m}+\boldsymbol{r}}^{(\mathrm{gs})} \rangle_J = 0$ if $\boldsymbol{r} \neq 0$. The correlated bonds induce a local ferro/antiferromagnetic order into the GS. When $a = 0$ the system is a ferro/antiferromagnet and the order is global. In the ferromagnetic case $s_{\boldsymbol{m}}^{(\mathrm{gs})} s_{\boldsymbol{m}+\boldsymbol{r}}^{(\mathrm{gs})} = 1$ and in the antiferromagnetic case $s_{\boldsymbol{m}}^{(\mathrm{gs})} s_{\boldsymbol{m}+\boldsymbol{r}}^{(\mathrm{gs})}$ alternates between plus and minus one. Therefore, the GS spin correlation can be estimated

by

$$G_{\mathrm{gs}}(\boldsymbol{r}) = \frac{1}{|\Lambda'|} \sum_{\boldsymbol{m} \in \Lambda'} \left(\frac{\hat{\sigma}(\boldsymbol{r}) + 1}{2} \right) \langle s_{\boldsymbol{m}}^{(\mathrm{gs})} s_{\boldsymbol{m}+\boldsymbol{r}}^{(\mathrm{gs})} \rangle_J , \qquad (9)$$

$$\hat{\sigma}(\boldsymbol{r}) = \sigma(r_1)\sigma(r_2) \text{ with } \sigma(r_i) = \begin{cases} 1 & \text{if } r_i \text{ is even} \\ -1 & \text{if } r_i \text{ is uneven} \end{cases}$$

and $\boldsymbol{r} = (r_1, r_2) \in \mathbb{Z}^2$. $\Lambda' \subset \Lambda$ is adjusted to the BCs. Note that this definition means that the correlation is measured for each site $\boldsymbol{m} \in \Lambda'$ on one of the two sub-lattices of a checkerboard partition of the square lattice, such that the correlation is insensitive to whether the order is ferromagnetic or antiferromagnetic.

In figure 9 one can see the GS correlation for different values of a. The data is well described by a scaling form of type

$$G_{\mathrm{gs}}(r) \sim \frac{1}{r^{\upsilon}} \exp \left\{ -\left(\frac{r}{\xi_{\mathrm{gs}}} \right)^{\varphi} \right\} . \qquad (10)$$

From the perspective of ordering we are especially interested in the correlation length, ξ_{gs}, that provides the distance in which spins are notably correlated. The straight forward method to extract ξ_{gs} is fitting the function of Eq. (10) to the data. The problem with such an approach is that neither υ nor φ are known. Also finite-size corrections reduce the match between scalingform and actual data. Thus, we used different approaches to obtain ξ_{gs}. First, we perform a separate *fit* for each value of a down to small correlations where the error bars start to exceed one quater of the correlation value. We observed that for $a \geq 2$, the values of the exponents υ and φ did not change much, for smaller values of a the exponents were a bit smaller. Therefore, we fixed the exponents to the (averaged) values seen for $a \geq 2$ and fitted only with respect to ξ_{gs}.

Second, we also performed a *multifit*, i.e., we fitted the correlation function simultaneously [54] with one value for υ, one value for φ and many values $\xi_{\mathrm{gs}} = \xi_{\mathrm{gs}}(a)$. The results of this multifit are also shown in Fig. 9. The obtained values for ξ_{gs} for these two fitting approaches are shown in Fig. 10. As visible the results from fixing the values of the exponents and from using the multifit approach do not differ much.

Befor we disuss the behavior of $\xi_{\mathrm{gs}}(a)$, we describe the third approach we have used to estimate the correlation length. Here, we used the *integral estimator* that was introduced in Ref. [55]. It presupposes that for $r \leq \xi_{\mathrm{gs}}$ the correlation function is dominated by a power law of type $r^{-\upsilon}$, whereas for $r > \xi_{\mathrm{gs}}$ the correlation is negligible. As a consequence, the integral

$$I_k = \int_0^{\infty} \mathrm{d}r \, r^k G_{\mathrm{gs}}(r) \qquad (11)$$

is given by $I_k \propto (\xi_{\mathrm{gs}})^{k+1-\upsilon}$ and thus

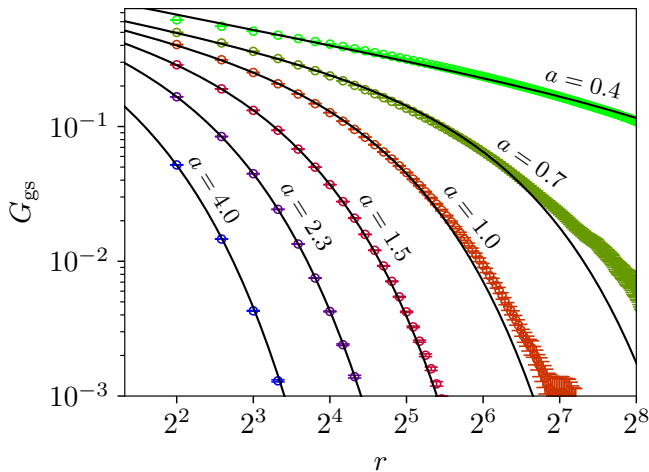$$\xi_{\mathrm{gs}}^{(k,k+1)} := \frac{I_{k+1}}{I_k} \propto \xi_{\mathrm{gs}} . \qquad (12)$$

FIG. 9. (color online) Spin correlation of the GS for different values of a. The correlation was computed by utilizing the estimator of Eq. (9) along the main axes. The black lines are fits according to Eq. (10) when using a multifit, i.e., fitting two exponents v and φ and many values of $\xi_{gs}(a)$ simultaneously to the correlation obtaiend for all values of a.

FIG. 10. (color online) The correlation length of the GS, $\xi_{gs}^{(1,2)}$, as a function of $1/a^2$, obgtained by three different approaches. For comparison the length scales $L^\star$ of the maxima are shown again.

This result would be exact and independent of k if the correlation acutally was only a power law. For real correlations, the value of k dictates which part of the correlation function contributes most to the integral. Because such a scaling approach is only valid when r is much larger than the lattice constant a high value of k reduces the systematic error of the method. On the other hand, large values of k increase the statistical error of I_k. Following the recommendation of [56] we used $\xi_{gs}^{(1,2)}$ as a compromise. Note that since the statistical error of the measured correlation grows with distance r, one usually defines a cutoff distance up to which the data is directly used for the integral. Similar to [56] we specified this cutoff distance as the value of r where G_{gs} is smaller than three times its error. For values of r larger than this cutoff distance we computed the integral up to the maximal length of L from fits to Eq. (10). The start value of these fits were set to $r_{min}^{(fit)} \geq 2$. Because it was observed that the correlation decays slightly different along the direction with free and periodic BCs, the computation of the GS were done with an independent set of simulations for full free BCs.

Afterwards, the correlation length $\xi_{gs}^{(1,2)}$ was extracted from the average of the GS correlation, G_{gs}, along the main axes. The statistical error of $\xi_{gs}^{(1,2)}$ was estimated by bootstrapping [54, 57] and the integrals according to Eq. (11) were computed by utilizing the midpoint integration rule. For small values of a, the contribution to I_k from the integral beyond the cutoff gets increasingly large. For instance, when $a = 1.15$ this contribution made up approximately 4% of the value of I_2. Hence, to estimate the total error, we added an extra systematical error to the statistical error. This was done by analyz-
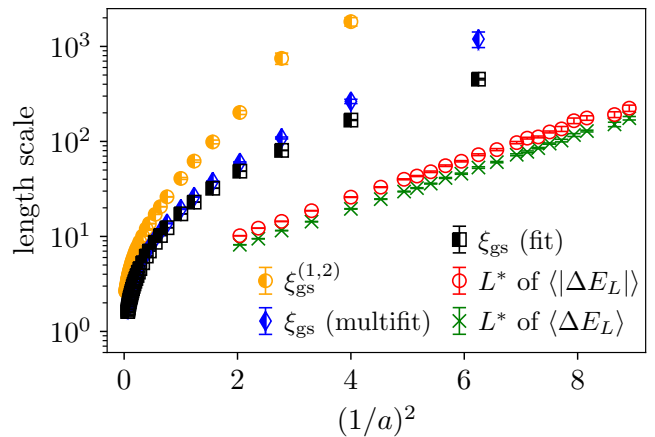
ing the value of $\xi_{gs}^{(1,2)}$ for two other choices of the the cutoff distance, i.e., being the the distance where the error of the correlation function is two or four times larger than its estimate, respectively. The maximal deviation of these two values from the standard definition, which uses a magnitude of three error bars to define cutoff, was set to be the systematic error. Furthermore, because the statistical error of I_k grows much large for small values of the correlatiopn exponent a and the system has to be sufficiently large to neglect boundary effects, values of $a < 1.15$ were not considered for this approach.

Figure 10 shows $\xi_{gs}^{(1,2)}$ as a function of the correlation exponent. As the plot demonstrates, the behavior does, in contrast to the data for the length scales $L^\star$, not follow a perfect exponential behavior. But for $a \to 0$ it also may converge to this behavior. We found that the data could be well fit to a function of type

$$\xi_{gs}^{(1,2)}(a) = A_\xi (a - a_{crit})^{-d_\xi} \exp\left\{ b_\xi (a - a_{crit})^{-c_\xi} \right\}, \quad (13)$$

to the data. The exponential in Eq. (13) is consistent with the previous results for the length scale $L^\star$ and will dominate for $a \to 0$. The power-law part is chosen to describe the behavior for large values of a. We have fitted the data to this function, e.g., for the data obtained from the multifit. Here, we again obtained a small value of $a_{crit} = 0.11(6)$, thus we again fixed $a_{crit} \equiv 0$. In this case we obtained as values of the remaining fit parameters $A_\xi = 4.0(3)$, $d_\xi = 0.81(3)$, $b_\xi = 1.58(8)$ and $c_\xi = 1.19(4)$ with a good quality of the fit. Similar values, in particular for c_ξ, are found for the other two data sets $\xi_{gs}(a)$. This means, for large correlation exponents a the behavior of the correlation length as function of a seems to be better described by a power law. Also, the behavior of the peak lengths and of the ferromagnetic correlation lengths differ a lot, but it is still possible that for very small values of a, the exponential dependence on $1/a^2$ is recovered for ξ_{gs}.

But to investigate this issue even much larger system sizes would have to be treated, much beyond the current numerical capabilities.

IV. DISCUSSION

The common two-dimensional Ising spins glass does not exhibit a finite-temperature spin glass phase in contrast to the three or higher dimensional cases [18–20]. This work deals with the question how long-range correlated bonds influence this characteristic. Therefore, the ordering behaviour of the two-dimensional Ising spin glass with spatially long-range correlated bonds is studied in the zero-temperature limit. The bonds are drawn from a standard normal distribution with a two-point correlation for bond distance r that decays as $(r^2 + 1)^{-a/2}$, $a \geq 0$. In the borderline case, when $a = 0$, the system is either a ferromagnet or antiferromagnet, depending on the bond realization. If $a \to \infty$ the uncorrelated EA model is recovered.

For $0 < a < \infty$ we observed that the correlation has local effects on the zero-temperature ordering behaviour. The correlation locally effects the average value of the bonds as well as their standard deviation for each individual realization of the disorder. These parameters are decisive to distinguish between a spin glass or ferro/antiferromagnet in case of the uncorrelated model [25, 28]. In correspondence to that, the spin correlation of the GS reveals how the correlation induces a local ferro/antiferromagnetic order into the GS. This is reflected by a growing correlation length $\xi_{\mathrm{gs}}(a)$ when decreasing a.

Complementary results, to the direct study of the GS, were obtained by investigating DW excitations. The absolute value of the DW energy can be interpreted as the coupling strength between block spins at zero temperature [14]. We found that for strong correlation the absolute value of the DW energy increases as a function of the system size to a peak and then decreases. Since we made the same observation for the actual DW energy it shows that the increase of the absolute value of the DW energy is a consequence of local ferro/antiferromagnetic order of the system in GS. The system size where the peak occurs, L^*, is interpreted as the length scale of local order. For small correlation exponents a, both $L^*(a)$ and the correlation length of the GS, $\xi_{\mathrm{gs}}(a)$, can be described by exponential divergencies, with correations for $\xi_{\mathrm{gs}}(a)$. Interestingly, a similar exponential length scale was also found in the two-dimensional random field Ising model by GS computations [49] and at low temperatures [48]. In these studies the length scale of ferromagnetic order was examined as a function of the standard deviation of the random magnetic field.

In case of the two-dimensional Ising spin glass the distribution of the absolute value of the domain wall energy is "universal" with respect to the initial bond distribution. This means for any continuous, symmetric bond distribution with sufficiently small mean and finite higher moments, the absolute value of the domain wall energy should approach the same scaling function [13, 14, 58]. Thus, we expect the same kind of universality for our model.

The stiffness exponent describes the scaling of the width of this distribution and is related via $\nu = -1/\theta$ to the only independent critical exponent of the thermal zero-temperature fixed point [14, 24]. Therefore, any correlation which leaves the stiffness exponent unchanged does not influence the universality of the model. From the data of L^* it is expected that there is no global ordered phase for $a > 0$. This implies that the stiffness exponent is negative for $a > 0$. Furthermore, for any considered $a \geq 0.9$ the stiffness exponent stays constant in comparison to the uncorrelated case. Due to the limited studied length scales it was not possible for us to verify this for the values of $a < 0.9$.

Beside the DW energy the DW surface is an essential parameter to describe the low-temperature behaviour of the Ising spin glass [50, 51]. In the uncorrelated model the domain-wall surface follows a power law, $\langle \mathcal{D} \rangle_J \sim L^{d_s}$, where $d_s = 1.27319(9)$ [21]. Our results are compatible to this for all considered correlation exponents $a \geq 0.5$. At $a \approx 0.4$ the fractal surface dimension starts to decline. For the values of $a \leq 0.1$ the data is well described by a power law with scaling corrections [16, 21], i.e. $\langle \mathcal{D} \rangle_J = A_{\mathcal{D}} L^{d_s}(1 + B_{\mathcal{D}} L^{-\omega_s})$. The decrease in the d_s implies that for strong correlations DWs with shorter lengths are energetic favorable. In the borderline case when $a = 0$ the system is a ferro/antiferromagnet and thus $d_s = 1$. Of course, it can not be ruled out that the decline in d_s is local and on sufficiently long length scales the pure power law with $d_s = 1.27319(9)$ [21] is recovered again for all $a > 0$. In this context it is interesting to note that there exist a relation which links directly the stiffness exponent with the the fractal surface dimension, i.e $d_s = 1 + 3/(4(3 + \theta))$ [59]. According to highly accurate numerical results [21] this equation is probably not correct. Our results for the fractal surface dimension $d_s = 1.27318(29)$ ($Q = 0.99$) and the stiffness exponent $\theta = -0.2815(13)$ ($Q = 0.13$) deviate by approximately 6.5 standard deviations from the mentioned conjecture, since $d_s - 1 - 3/(4(3+\theta)) = -0.0027(4)$. The latter result was obtained by using standard error propagation, thus, neglecting correlations between the estimates of d_s and θ which exist because both values were obtained from the same data set. In any case, our results also rather support that the proposed scaling relation does not hold.

In conclusion, it is observed that the correlation has strong effect on the ordering on local length scales, inducing ferro/antiferromagnetic domains into the GS. The length scale of local ferro/antiferromagnetic order diverges exponentially when the correlation exponent approaches zero. The fractal surface dimension decreases for strong correlations on the studied length scales. No sign of a spin-glass phase at finite temperature is witnessed.

[1] E. Vincent and V. Dupuis, in *Frustrated Materials and Ferroic Glasses*, edited by T. Lookman and X. Ren (Springer, Cham, 2018) pp. 31–56.

[2] S. F. Edwards and P. W. Anderson, J. Phys. F **5**, 965 (1975).

[3] D. Sherrington and S. Kirkpatrick, Phys. Rev. Lett. **35**, 1792 (1975).

[4] D. L. Stein and C. M. Newman, *Spin Glasses and Complexity* (Princeton University Press, Princeton, 2013).

[5] M. Mézard, G. Parisi, and M. Virasoro, *Spin Glass Theory and Beyond* (World Scientific, Singapore, 1987).

[6] A. P. Young, ed., *Spin Glasses and Random Fields* (World Scientific, Singapore, 1998).

[7] E. Bolthausen and A. Bovier, eds., *Spin Glasses* (Springer, Berlin, Heidelberg, 2007).

[8] H. Nishimori, *Statistical Physics of Spin Glasses and Information Processing: An Introduction* (Oxford University Press, Oxford, 2001).

[9] V. Dotsenko, *An introduction to the theory of spin glasses and neural networks* (World Scientific, Singapore, 1994).

[10] A. K. Hartmann and H. Rieger, *Optimization Algorithms in Physics* (Wiley-VCH, Weinheim, 2002).

[11] A. K. Hartmann and H. Rieger, eds., *New Optimization Algorithms in Physics* (Wiley-VCH, Weinheim, 2004).

[12] Z. Zhu, A. J. Ochoa, and H. G. Katzgraber, Phys. Rev. Lett. **115**, 077201 (2015).

[13] W. McMillan, J. Phys. C **17**, 3179 (1984).

[14] A. Bray and M. Moore, in *Heidelberg Colloquium on Glassy Dynamics*, edited by J. van Hemmen and I. Morgenstern (Springer, Berlin, Heidelberg, 1987) pp. 121–153.

[15] D. S. Fisher and D. A. Huse, Phys. Rev. B **38**, 386 (1988).

[16] A. K. Hartmann and M. A. Moore, Phys. Rev. Lett. **90**, 127201 (2003).

[17] A. K. Hartmann and M. A. Moore, Phys. Rev. B **69**, 104409 (2004).

[18] A. P. Young and R. B. Stinchcombe, J. Phys. C **9**, 4419 (1976).

[19] B. Southern and A. P. Young, J. Phys. C **10**, 2179 (1977).

[20] A. K. Hartmann and A. P. Young, Phys. Rev. B **64**, 180404 (2001).

[21] H. Khoshbakht and M. Weigel, Phys. Rev. B **97**, 064410 (2018).

[22] F. Parisen Toldin, A. Pelissetto, and E. Vicari, Phys. Rev. E **84**, 051116 (2011).

[23] C. K. Thomas, D. A. Huse, and A. A. Middleton, Phys. Rev. Lett. **107**, 047203 (2011).

[24] L. Fernandez, E. Marinari, V. Martin-Mayor, G. Parisi, and J. Ruiz-Lorenzo, Phys. Rev. B **94**, 024402 (2016).

[25] D. Sherrington and W. Southern, J. Phys. F **5**, L49 (1975).

[26] C. Amoruso and A. K. Hartmann, Phys. Rev. B **70**, 134425 (2004).

[27] R. Fisch and A. K. Hartmann, Phys. Rev. B **75**, 174415 (2007).

[28] C. Monthus and T. Garel, Phys. Rev. B **89**, 184408 (2014).

[29] H. Fajen, A. K. Hartmann, and A. P. Young, Phys. Rev. E **102**, 012131 (2020).

[30] A. Weinrib and B. I. Halperin, Phys. Rev. B **27**, 413 (1983).

[31] B. Ahrens and A. K. Hartmann, Phys. Rev. B **84**, 144202 (2011).

[32] T. Nattermann, in *Spin Glasses and Random Fields*, edited by A. P. Young (World Scientific, Singapore, 1998) pp. 277–298.

[33] H. A. Makse, S. Havlin, M. Schwartz, and H. E. Stanley, Phys. Rev. E **53**, 5445 (1996).

[34] J. W. Cooley and J. W. Tukey, Mathematics of Computation **19**, 297 (1965).

[35] M. Frigo and S. G. Johnson, Proceedings of the IEEE **93**, 216 (2005).

[36] C. Newman and D. Stein, Phys. Rev. Lett. **84**, 3966 (2000).

[37] L.-P. Arguin and M. Damron, Annales de l'I.H.P. Probabilités et statistiques **50**, 28 (2014).

[38] A. K. Hartmann, in *Rugged Free Energy Landscapes*, edited by W. Janke (Springer, Berlin, Heidelberg, 2008) pp. 67–106.

[39] F. Barahona, J. Phys. A **15**, 3241 (1982).

[40] L. Bieche, J. Uhry, R. Maynard, and R. Rammal, J. Phys. A **13**, 2553 (1980).

[41] F. Barahona, R. Maynard, R. Rammal, and J. Uhry, J. Phys. A **15**, 673 (1982).

[42] G. Pardella and F. Liers, Phys. Rev. E **78**, 056705 (2008).

[43] C. K. Thomas and A. A. Middleton, Phys. Rev. B **76**, 220406 (2007).

[44] W. Cook and A. Rohe, INFORMS Journal on Computing **11**, 138 (1999).

[45] A. Rohe, "The Blossom Four Code for Min-Weight Perfect Matching," https://www.math.uwaterloo.ca/ bico/blossom4/.

[46] A. C. Carter, A. J. Bray, and M. A. Moore, Phys. Rev. Lett. **88**, 077201 (2002).

[47] A. K. Hartmann, A. J. Bray, A. C. Carter, M. A. Moore, and A. P. Young, Phys. Rev. B **66**, 224401 (2002).

[48] E. Pytte and J. Fernandez, J. Appl. Phys. **57**, 3274 (1985).

[49] E. Seppälä, V. Petäjä, and M. J. Alava, Phys. Rev. E **58**, R5217 (1998).

[50] A. J. Bray and M. A. Moore, Phys. Rev. Lett. **58**, 57 (1987).

[51] C. M. Newman and D. L. Stein, in *Spin glasses*, edited by E. Bolthausen and A. Bovier (Springer, Berlin, Heidelberg, 2007) pp. 145–158.

[52] N. Kawashima, J. Phys. Soc. Jpn. **69**, 987 (2000).

[53] O. Melchert and A. K. Hartmann, Phys. Rev. B **76**, 174411 (2007).

[54] A. K. Hartmann, *Big Practical Guide to Computer Simulations* (World Scientific, Singapore, 2015).

[55] F. Belletti, M. Cotallo, A. Cruz, L. Fernandez, A. Gordillo-Guerrero, M. Guidetti, A. Maiorano, F. Mantovani, E. Marinari, V. Martin-Mayor, *et al.*, Phys. Rev. Lett. **101**, 157201 (2008).

[56] F. Belletti, A. Cruz, L. Fernandez, A. Gordillo-Guerrero, M. Guidetti, A. Maiorano, F. Mantovani, E. Marinari, V. Martin-Mayor, J. Monforte, *et al.*, J. Stat. Phys. **135**, 1121 (2009).

[57] A. P. Young, *Everything You Wanted to Know About Data Analysis and Fitting but Were Afraid to Ask* (Springer, Cham, 2015).

[58] C. Amoruso, E. Marinari, O. C. Martin, and A. Pagnani, Phys. Rev. Lett. **91**, 087201 (2003).

[59] C. Amoruso, A. K. Hartmann, M. B. Hastings, and M. A. Moore, Phys. Rev. Lett. **97**, 267202 (2006).